ZNF280A Promotes Lung Adenocarcinoma Development through Regulating the Expression of EIF3C

Hongsheng Liu
Department of Thoracic Surgery, Peking Union Medical College Hospital
Yingzhi Qin
Department of Thoracic Surgery, Peking Union Medical College Hospital
Na Zhou
Department of Medical Oncology, Peking Union Medical College Hospital
Dongjie Ma
Department of Thoracic Surgery, Peking Union Medical College Hospital
Yingyi Wang (lhsheng2020@163.com)
Peking Union Medical College Hospital https://orcid.org/0000-0001-9295-0465

Research

Keywords: Lung cancer, ZNF280A, EIF3C, RNA sequencing, tumor promotor

Posted Date: May 5th, 2020

DOI: https://doi.org/10.21203/rs.3.rs-26101/v1

Abstract

Background: Lung cancer is the most commonly diagnosed malignant tumor worldwide. Lung adenocarcinoma (LUAD) is the most common histological subtype in non-small cell lung cancer (NSCLC). The relationship between ZNF280A and LUAD has not been demonstrated and remains unclear.

Methods: In this study, it was demonstrated that ZNF280A was upregulated in LUAD tissues compared with the normal tissues. Further investigations indicated that the overexpression/knockdown of ZNF280A could promote/inhibit proliferation, colony formation and migration of LUAD cells, while inhibiting/promoting cell apoptosis. Moreover, knockdown of ZNF280A could also suppress tumorigenicity of LUAD cells *in vivo*. RNA-sequencing followed by Ingenuity pathway analysis (IPA) was performed for exploring downstream of ZNF280A and identified EIF3C as the potential target.

Results: Furthermore, our study revealed that knockdown of EIF3C could inhibit development of LUAD *in vitro*, and alleviate the ZNF280A overexpression induced promotion of LUAD.

Conclusions: In conclusion, our study showed, as the first time, ZNF280A as a tumor promotor for LUAD, whose function was carried out probably through the regulation of EIF3C.

Background

Lung cancer is the leading cause of cancer-related incidents and mortality worldwide, which is malignant neoplasm of the respiratory system [1,2]. According to histological classification, lung cancer can be divided into small cell lung cancer (SCLC) and non-small cell lung cancer (NSCLC) [3,4], among which NSCLC is the most common histopathological type and lung adenocarcinoma (LUAD) is the most common histological subtype in NSCLC [5]. Despite the recent improvements of modern medicine and therapeutic strategies of lung cancer treatment, patients with LUAD still suffer from an extremely poor prognosis, whose 5-year survival rate is only approximate 20% [6]. Late diagnosis and insufficient efficiency of current therapy are the major cause of the poor prognosis of LUAD patients [7]. Therefore, the exploration of novel key regulatory molecules involved in the development and progression of LUAD could provide valuable candidate for more effective molecular targeted therapies, benefitting for LUAD patients [8–10].

Zinc finger protein is a type of transcription factor with a special "finger-like" domain, which usually exists in various eukaryotes and possesses the function of regulating and controlling gene expression [11]. The most representative characteristic of zinc finger protein family members is that they can produce a short stereoscopic structure model of polypeptide according to their own folding pattern, and maintain the stability of such molecular structure by combining with zinc ions [11]. It has been revealed that zinc finger protein plays critical role in embryonic development, cell differentiation, signal transduction and, especially, the development and progression of human cancers [12]. For example, ZNF280B was identified as a potential mechanism of p53 suppression in prostate cancer, which promoted the development of

prostate cancer. ZNF280A, which encodes a zinc finger protein with C_2H_2 motif, was found to be potentially involved in mantle cell lymphoma [13]. However, the relationship between ZNF280A and most types of human cancers including LUAD remains unclear.

In this study, relatively high expression of ZNF280A was observed in lung cancer tissues in comparison with normal tissues, which was significantly correlated with more serious disease and poorer prognosis. Loss-of-function and gain-of-function studies revealed the regulatory role of ZNF280A in the development and progression of LUAD by influencing cell proliferation, colony formation, cell apoptosis, cell cycle distribution and cell migration. The xenografts formed by inoculation of cells with ZNF280A knockdown progress much slower relative to the control group. Furthermore, EIF3C was screened as the potential downstream of ZNF280A to mediate the regulation of LUAD development. In a word, this study identified ZNF280A as an oncogene-like factor in the development of LUAD, which may be used as an effective therapeutic target in LUAD treatment.

Materials And Methods

Cell lines and cell transfection

A549 and NCI-H1299 cells were purchased from the Cell Bank of Type Culture Collection of Chinese Academy of Sciences and NCI-H1299 were cultured in RPMI-1640 medium (Gibco) with 10% FBS and A549 was maintained in McCoy's 5A Medium with 10% FBS. All cells were cultured in a humidified cell culture incubator at 37 °C under 5% CO_2 with culture medium changed every 72 h.

For stable gene expressing, lipofectamine RNAimax (Cat. #13778075, Thermo fish) were used for cell A549 and NCI-H1299 transfection with lentiviral plasmids collected. Cells were harvested after 72 h culturing, and cell infection efficiency was valued with LV-shCtrl cells as control.

Immunohistochemical (ihc) Staining

Human lung cancer and para-normal tissue chip (Cat. #HLugA180Su05, Shanghai Outdo Biotech Company) was used and patients' information was collected. For IHC staining, deparaffinized and rehydrated tissue sections were blocked and incubated with primary antibody ZNF280A (Cat. #bs-12839R, BIOSS) and followed incubated by secondary antibody. DAB color was developed with diaminobenzene and hematoxylin. Slides were pictured with microscopic and viewed with ImageScope and CaseViewer. All slides were examined randomly by two independent pathologists and IHC outcomes were determined by staining percentage and intensity scores. Staining percentage scores were classified as: 1 (1%-24%), 2 (25%-49%), 3 (50%-74%) and 4 (75%-100%). Staining intensity were scored 0 (Signalless color) to 3 (light yellow, brown and dark brown). Antibodies used in IHC were listed in Table S1.

Rna Interference And Plasmids Packaging

shRNA sequences targeting human ZNF280A and EIF3C gene were designed and cDNAs were synthesized by Shanghai Yibeirui Bioscienceres, Co., Ltd. and subsequently cloned into luciferase-labelled BR-V-108 vector. In addition, ZNF280A was amplified and cloned into the BR-V112 vector after double digestion by BamHI and AgeI, and sequenced. Lentiviral particles were collected, following co-transfection using pHelper 1.0 and pHelper 2.0 vector for plasmids packaging. The sequences used were listed in Table S2.

Rna Extraction And Rt-qpcr

After 72 h for ZNF280A and/or EIF3C RNA expressing, A549 and NCI-H1299 cells in triplicate were fully lysed and total RNA was extracted using TRIzol reagent (Sigma). The RNA quality was evaluated by Nanodrop 2000/2000C spectrophotometer (Thermo Fisher Scientific). cDNA was reversely transcribed from RNA using Promega M-MLV Kit (Promega) and qPCR was performed with SYBR Green mastermixs Kit (Vazyme) by applying Biosystems 7500 Sequence Detection system. GAPDH was acted as inner control, and the primers used for the PCR reaction were showed in Table S3. The relative quantitative analysis in gene expression data were analyzed by the $2^{-\Delta\Delta Ct}$ method.

Western blotting (WB), co-immunoprecipitation (Co-IP) and Human Apoptosis Antibody Array

Cells were lysed in ice-cold RIPA buffer (Millipore), and the protein were collected and the concentration was detected by a BCA Protein Assay Kit (HyClone-Pierce). Protein samples (20 μg per lane) were separated by 10% SDS-PAGE (Invitrogen), and transferred onto PVDF membranes at 4 °C. The membranes were blocked with TBST solution of 5% degreased milk at room temperature for 1 h and incubated with primary antibodies and GAPDH antibodies at 4 °C overnight. Then the membranes were incubated with secondary antibody HRP goat anti-rabbit IgG for 2 h at room temperature. The blots were visualized by enhanced chemiluminescence (ECL) (Amersham).

For Co-IP, prepared proteins were immunoprecipitated by anti-ZNF280A, EIF3C or GAPDH antibody and then subjected to WB with antibody to ZNF280A and EIF3C and related secondary antibodies.

For Human Apoptosis Antibody Array, briefly, 20 μg total proteins were cultured with the antibody-coated array membranes and then continuing incubated with HRP linked Streptavidin conjugate.

All the antibodies used in western blotting were listed in Table S1.

Cell Proliferation Analysis

The cell viability was determined by MTT assay, briefly, transfected A549 and NCI-H1299 cells were stained with MTT reagent (5 mg/mL, GenView) and Formazan was dissolved by DMSO solution. The

absorbance values at 490 nm were measured by microplate reader (Tecan) and the reference wavelength was 570 nm.

Cell proliferation rate was analyzed by Celigo cell counting assay. Briefly, targeting cells were seeded at a 96-well plate with 2,000 cells per well. The plate was continuously detected by Celigo (Nexcelom) for 5 days at the same time.

For colony formation assay, cells in the logarithmic growth phase were seeded into 6-well plates in triplicate and further cultured for 8 days. Cell clones were fixed with 4% paraformaldehyde and stained with Giemsa. Then clones were photographed under a fluorescence microscope (Olympus) and colony number (clone contains more than 50 cells) was counted.

Cell Apoptosis And Cells Cycle Assay

The flow cytometric methods of identifying apoptotic cells was applied using Annexin V-APC Apoptosis kit (Cat. #88-8007, eBioscience). For cells cycle assay, cells were stained with 1 mL PI staining solution (40 × PI, 2 mg/mL: 100 × RNase, 10 mg/mL: 1 × PBS = 25:10:1000). FACScan and FlowJo 7.6.1 (Ashland) was used for analyze. Cell apoptosis was measured and the percentage of the cells in G0-G1, S, and G2-M phase were counted and compared.

Cell Migration Assays

In order to analysis the migration ability of transfected cells in our research, wound healing assay and Transwell assay were performed. For wound healing assay, lentivirus transfected A549 and NCI-H1299 cells (5×10^4 cells/well) were plated into 96-well plates for culturing. Scratches were made by a 96 wounding replicator (VP scientific). Photographs were taken by a fluorescence microscope at 0 h, 8 h and 24 h and cell locations were recorded, respectively. Cell migration rates of each cell group were calculated. In transwell assay, cells were seeded into a 24-well plate in the upper chambers, and medium supplemented with 30% FBS was added into in the lower chambers. Cells were fixed with 4% formaldehyde and stained by Giemsa and the migration ability of cells was analyzed.

High-throughput Rna Sequencing

Total RNA from NCI-H1299-shCtrl and NCI-H1299-shZNF280A cells was extracted using TRIzol. RNA quantity and quality were assessed with a Thermo Nanodrop 2000 ($1.7 < A260/A280 < 2.2$, Thermo Fisher Scientific). Affymetrix PrimeView Human Gene Expression Arrays (Thermo Fisher Scientific) were used for microarray analysis to obtain gene expression profiles according to the manufacturer's instructions. Significantly differentially expressed genes were selected based on $P < 0.05$ and $|\text{Fold Change}| > 1.3$. KEGG pathway enrichment analysis was performed for all significant differentially expressed genes.

Animal Experiments

All animal studies were approved by Ethics committee of Peking Union Medical College Hospital. Female BALB/c nude mice were purchased from Shanghai Lingchang Experimental Animals Co., Ltd. For tumorigenicity, 5×10^6 lentivirus (shCtrl or shZNF280A) transfected NCI-H1299 cells were subcutaneously injected into each mouse (4-week-old, n = 10 per group). Mice's weight and tumor sizes were recorded 2 times per week and the volume of tumor were calculated as $\pi/6 \times L \times W^2$ (W, width at the widest point; L, perpendicular width). Finally, the tumor burden was assessed by bioluminescence imaging with non-invasive IVIS Spectrum Imaging System (Perkin Elmer). Mice were sacrificed then tumors were extracted and imaged.

Ki67 Immunostaining Assay

Mice tumor sections were fixed in 4% paraformaldehyde. Paraffin embedded 5 μm sections were made for H&E and IHC staining. We added citric acid buffer for antigen retrieval at 120 °C. Sections were blocked using PBS-H_2O_2 with 0.1% Tween 20. Ki-67 antibody was added for incubating at 4 °C overnight and then secondary antibodies were added as well. DAB color was developed with diaminobenzene and hematoxylin. Stained slides were pictured with a microscopic.

Statistical Analyses

Each experiment was repeated three times and the data was shown as mean ± SD. Categorical variables were expressed as percentages. The significance between groups was determined using the two-tailed Student's t test or one-way ANOVA analysis. Relationship between ZNF280A expression and tumor characteristics in lung cancer patients with was analyzed using Mann-Whitney U analysis and Spearman grade correlation analysis. Statistical significance was calculated by SPSS 22.0 (IBM) and P value < 0.05 was considered statistically significant. Graphs were made using GraphPad Prism 6.01 (Graphpad Software).

Results

ZNF280A is upregulated in LUAD tissues and expressed in LUAD cells

For the sake of exploring the role of ZNF280A in LUAD, IHC analysis was employed to tell the difference in the expression of ZNF280A in LUAD tissues and normal tissues, indicating the upregulated expression of ZNF280A in LUAD (Fig. 1A). The statistical analysis of expression data collected from 92 LUAD tissues and 70 normal tissues also exhibited the generally higher expression of ZNF280A in LUAD ($P < 0.001$, Table 1). Correlation analysis between ZNF280A expression and clinical characteristics of patients with

LUAD revealed that ZNF280A expression was significantly upregulated in patients with more advanced tumor grade, tumor stage and higher risk of lymphatic metastasis ($P < 0.05$, Fig. 1A and Table 2), which could also be further verified by performing Spearman rank correlation analysis (Table S4). Consistently, Kaplan-Meier survival analysis revealed the poorer prognosis of LUAD patients with relatively higher ZNF280A expression (Fig. 1B). Additionally, based on the detection of endogenous expression of ZNF280A in LUAD cell lines, A549 and NCI-H1299 cells with relatively high ZNF280A expression was selected for constructing ZNF280A knockdown cell model for subsequent investigations (Fig. 1C).

Table 1
Expression patterns of ZNF280A in lung cancer tissues and normal tissues revealed in immunohistochemistry analysis

ZNF280A expression	**Tumor tissue**		**Normal tissue**	
	Cases	**Percentage**	**Cases**	**Percentage**
Low	42	45.7%	70	100%
High	50	54.3%	0	/
$P < 0.001$				

Table 2
Relationship between ZNF280A expression and tumor characteristics in patients with lung cancer

Features	No. of patients	ZNF280A expression		*P* value
		low	high	
All patients	92	42	50	
Age (years)				0.096
≤ 61	46	17	29	
> 61	46	25	21	
Gender				0.169
Male	51	20	31	
Female	41	22	19	
Tumor size				0.077
< 4 cm	39	22	17	
≥ 4 cm	53	20	33	
Lymph node positive				0.006
< 1	38	23	15	
≥ 1	51	16	35	
Grade				0.001
I	3	3	0	
II	61	33	28	
III	28	6	22	
Stage				0.011
1	27	18	9	
2	17	7	10	
3	42	13	29	
4	1	1	0	
T Infiltrate				0.038
T1	19	13	6	
T2	51	21	30	

Features	No. of patients	ZNF280A expression		*P* value
		low	high	
T3	16	7	9	
T4	6	1	5	
lymphatic metastasis (N)				0.016
N0	38	23	15	
N1	16	6	10	
N2	16	2	14	
N3	4	3	1	
Expession of EGFR (FISH)				0.944
Negative	72	34	38	
Positive	13	6	7	

ZNF280A knockdown inhibited LUAD development *in vitro*

ZNF280A deficiency cell model was constructed through the transfection of lentivirus designed for silencing ZNF280A to elucidate its detailed function in LUAD. The fluorescence signal observed in > 80% cells proved the successful infection (Figure S1), and the significant downregulation of ZNF280A mRNA and protein levels detected by qPCR ($P < 0.001$) and western blotting (Fig. 2A), respectively, confirmed the successful knockdown of ZNF280A in both cell lines. The outcomes of MTT assay showed that cells with ZNF280A depletion (shZNF280A) grew much slower than that without ZNF280A depletion (shCtrl) ($P < 0.001$, Fig. 2B). As another key factor in cell proliferation, cell apoptosis of LUAD cells with or without ZNF280A knockdown was evaluated by flow cytometry. As expected, cells with ZNF280A deficiency showed much bigger apoptotic cell population in comparison with shCtrl group ($P < 0.001$, Fig. 2C). Moreover, the detection of cell cycle distribution demonstrated that downregulation of ZNF280A in A549 and NCI-H1299 cells arrested cell cycle in G2 phase ($P < 0.001$, Fig. 2D). Otherwise, in order to expound the mechanism of ZNF280A to regulate cell apoptosis, an antibody array was performed to distinguish the influenced apoptosis-related proteins by ZNF280A. It was demonstrated that ZNF280A depletion induced the expression upregulation of Caspase3, Fas, HSP60, IGFBP-6, TNF-β, TRAILR-1 and TRAILR-2, and downregulation of Bcl-2, CD40, IGF-II, Livin and Survivin ($P < 0.05$, Figure S2). Furthermore, we employed wound-healing and Trasnswell assays to potentiate the decreased cell mobility of A549 and NCI-H1299 cells in shZNF280A groups ($P < 0.001$, Fig. 2F). Altogether, we supposed that ZNF280A may play a vital role in the development of LUAD through regulating cell apoptosis, colony formation, cell apoptosis and cell migration.

ZNF280A knockdown inhibited tumor growth of LUAD *in vivo*

After successfully constructing and culturing mice model through injection of NCI-H1299 cells with or without ZNF280A knockdown, the results of *in vivo* bioluminescence imaging showed markedly weaker total bioluminescence intensity, as well as smaller tumor burden, in shZNF280A group ($P < 0.001$, Fig. 3A-3B). Moreover, the smaller volume and lighter weight of solid tumors in the shZNF280A group also suggested that tumor growth slowed down upon silence of ZNF280A ($P < 0.001$, Fig. 3C-3E). Consistently, the lower Ki67 index, as well as lower proliferative activity, detected in the tumors removed from mice of shZNF280A groups further explained the above observations (Fig. 3F).

The potential of EIF3C as the downstream of ZNF280A in the regulation of LUAD

Given the basically clear regulatory role of ZNF280A in LUAD, we still wondered the underlying mechanism. Therefore, a 3 v 3 RNA-seq was conducted to identify differentially expressed genes (DEGs) between cells in shZNF280A group and shCtrl group of NCI-H1299 cells. Based on the threshold of simultaneous $|\text{Fold Change}| \geq 1.3$ and $\text{FDR} < 0.05$ (the *P* value after Benjamini-Hochberg analysis), 2735 DEGs were found to be upregulated in shZNF280A cells compared with shCtrl cells and 3515 DEGs were downregulated (Figure S3A-S3B). The enrichment of all the 6250 DEGs in canonical signaling pathway or IPA disease and function was assessed by IPA analysis (Figure S3C-S3D). Based on all the bioinformatics and the IPA based analysis of ZNF280A-associated interaction network, several DEGs with highest expression fold change were subjected to verification by qPCR and western blotting in HCCC-9810 cells (Fig. 4A-4D). Among them, EIF3C was supposed to be a promising candidate as the target of ZNF280A. Noteworthy, the expression of EIF3C showed a similar pattern with ZNF280A in LUAD tissues: higher expression in LUAD tissues than normal tissues (Fig. 4E). More specifically, the direct interaction between ZNF280A and EIF3C was clearly indicated by co-IP in NCI-H1299 cells, which was shown in Fig. 4F. In a word, EIF3C was identified as a potential target of ZNF280A during regulating LUAD, which would be further verified by *in vitro* investigations.

Knockdown of EIF3C blocked development of LUAD *in vitro*

In order to illuminate the role of EIF3C in LUAD, EIF3C knockdown cell model was constructed and verified using similar method as mentioned above. Among three shRNAs designed for EIF3C knockdown, RNAi-11091 was shown to possess the highest knockdown efficiency and utilized in subsequent experiments ($P < 0.001$, Figure S4A-S4B). After further verification of EIF3C knockdown by qPCR and western blotting (Fig. 5A-5B), NCI-H1299 cells with or without EIF3C knockdown were subjected to Celigo cell counting assay which showed the significantly restrained cell proliferation by EIF3C knockdown ($P < 0.001$, Fig. 5C). Consistently, we also found that knockdown of EIF3C significantly suppressed the colony

formation ability of NCI-H1299 cells ($P < 0.001$, Fig. 5D). Similar with ZNF280A knockdown, an 8.5-fold elevation of cell apoptosis rate by EIF3C knockdown could be observed in NCI-H1299 cells ($P < 0.001$, Fig. 5E). More importantly, it was demonstrated by wound-healing and Transwell assays that knockdown of EIF3C could significantly inhibit cell migration ability of NCI-H1299 cells ($P < 0.001$, Fig. 5F and 5G). Therefore, it could be concluded that knockdown of EIF3C exhibited similar inhibition effects on LUAD with ZNF280A knockdown.

Eif3c Knockdown Alleviated Znf280a Overexpression Induced Promotion Of Luad

In order to clarify the synergistic effect of ZNF280A and EIF3C on LUAD, NCI-H1299 cells with ZNF280A overexpression or simultaneous ZNF280A overexpression and EIF3C knockdown were constructed. The effects of ZNF280A overexpression on functions of NCI-H1299 cells were preliminarily investigated following the detection of transfection efficiency (> 80%, Figure S5A) by fluorescent imaging and verification of knockdown efficiency by qPCR and western blotting ($P < 0.001$, Figure S5B-S5C). It was demonstrated that ZNF280A overexpression significantly promoted proliferation ($P < 0.001$, Fig. 6A) and colony formation ability ($P < 0.001$, Fig. 6B) of NCI-H1299 cells, which was in contrast with the results of ZNF280A and EIF3C knockdown. Interestingly, ZNF280A overexpression only exhibited ignorable influence on cell apoptosis of NCI-H1299 cells without statistical significance (Fig. 6C). Furthermore, we also found that ZNF280A overexpression significantly promoted cell migration ability of NCI-H1299 cells in both wound-healing and Transwell assays ($P < 0.01$, Fig. 6D and 6E). On the other hand, successful transfection, upregulation of ZNF280A and downregulation of EIF3C were also proved in NCI-H1299 of ZNF280A + shEIF3C group ($P < 0.05$, Figure S6). An overall inhibition effect on cell proliferation was observed with simultaneous ZNF280A overexpression and EIF3C knockdown ($P < 0.001$, Fig. 6A). Moreover, subsequent experiments showed that the effects of ZNF280A overexpression on colony formation ($P < 0.001$, Fig. 6B), cell apoptosis ($P < 0.05$, Fig. 6C) and cell migration ($P < 0.01$, Fig. 6D for wound-healing assay and 6E for Transwell assay) could be attenuated or even reversed by EIF3C knockdown. In a word, these results suggested that ZNF280A may execute regulatory effects on LUAD through the regulation of EIF3C.

Discussion

Zinc finger proteins are a group of transcription factors with special finger-like domains. They can generate finger-like structures by self-folding and bind to zinc ions to maintain stability [14]. In the past decades, accumulating evidence indicated that zinc finger proteins were involved in the development and progression of various human cancers [12]. For example, study of Li *et al.* indicated that ZNF677 could transcriptionally suppress the expression of CDKN3 and HSPB1, thus inhibiting the activation, as well as phosphorylation of Akt and the tumorigenesis of thyroid cancer [15]. Nie *et al.* identified ZNF139 as target of miR-195-5p in the multi-drug resistance of gastric cancer [16]. ZNF668 was reported to be capable of

suppressing the invasion and migration of non-small cell lung cancer through regulation of EMT related factors [17]. In bladder cancer, a member of zinc finger protein family ZNF224 was found to form complex with DEPDC1, inhibition of which could potentially repress bladder carcinogenesis [18].

In this study, the relationship between LUAD and ZNF280A, which is rarely investigated in the development of cancer, was studied. The IHC analysis of clinical specimens clarified the upregulated expression of ZNF280A was observed in tumor tissues of LUAD. Moreover, knockdown of ZNF280A significantly inhibited cell proliferation of LUAD, and promoted cell apoptosis through the upregulation of Caspase3, Fas, HSP60, IGFBP-6, TNF-β, TRAILR-1 and TRAILR-2, and downregulation of Bcl-2, CD40, IGF-II, Livin and Survivin. The promotion effects of ZNF280A knockdown on cell apoptosis could also be attributed to the arrest of cell cycle in G2 phase by ZNF280A knockdown. Besides, we also found that ZNF280A overexpression exhibited conversed effects against ZNF280A knockdown on cell proliferation and colony formation ability, while simultaneously promoting cell migration of LUAD cells. All these results recognized ZNF280A as a tumor promotor in the development and metastasis of LUAD. Furthermore, the role of ZNF280A in LUAD was finally proved by *in vivo* experiments, which showed significantly restrained tumor growth of LUAD upon ZNF280A knockdown.

Eukaryotic initiation factor 3 (EIF3) is a multi-subunit complex, which was first isolated and purified from rabbit reticulocytes [19]. The EIF3 family of mammals is composed of 13 members, EIF3A~EIF3M. EIF3 subunits are usually located in the cytoplasm, while EIF3A, EIF3E and EIF3K can participate in the regulation of protein translation between cytoplasm and nucleus due to their special structure [20]. In the process of eukaryotic cell translation initiation, EIF3 can bind directly to small 40S ribosome subunits, thus promoting the formation of the eukaryotic initiation factor 2-triphosphate-amino acid-tRNA (Met-tRNA) ternary complex of the 43S subunit precursor complex, and regulating the synthesis of protein in the process of protein translation [21]. Recent studies showed that EIF3 plays an important role in the occurrence and development of malignant tumors [22,23]. For example, EIF3A, the largest subunit of EIF3 family, is highly expressed in various malignant tumor tissues and has been used as a potential target for anti-cancer drugs [24]. As one of the core subunits of EIF3, EIF3C was also demonstrated to be involved in the development and progression of several types of malignant tumors such as ovarian cancer [25,26], renal cell carcinoma [27], osteosarcoma [28] and cervical cancer [29]. However, the association between EIF3C and LUAD is still not clear and rarely reported.

Herein, we found that EIF3C knockdown could significantly inhibit cell proliferation and colony formation of LUAD cells, while promoting cell apoptosis. Moreover, EIF3C knockdown also suppressed cell migration of LUAD cells. More importantly, the investigation of the synergistic effects of ZNF280A and EIF3C on LUAD showed that EIF3C knockdown could alleviate or even reversed the regulation of LUAD by ZNF280A overexpression. All the results showed the role of EIF3C as a tumor promotor in LUAD and a potential target of ZNF280A.

In conclusion, we found the upregulated expression of ZNF280A and EIF3C in tumor tissues of LUAD. Both ZNF280A and EIF3C could act as tumor promotors in the development and progression of LUAD, through regulation cell proliferation, colony formation, cell apoptosis and cell migration. More importantly, EIF3C knockdown could attenuate ZNF280A overexpression-induced promotion of LUAD. Therefore, the regulation of LUAD by ZNF280A through EIF3C make it a potential therapeutic target for LUAD treatment.

Declarations

Ethics approval and consent to participate

All animal studies were approved by Ethics committee of Peking Union Medical College Hospital.

Consent for publication

Not applicable.

Availability of data and materials

Not applicable.

Competing interests

The authors declare that they have no competing interests.

Funding

This study was financially supported by CAMS Initiative for Innovative Medicine (CAMS-2017-I2M-4-002), National Natural Science Foundation of China (No. 61435001), CAMS Innovation Fund for Medical Sciences(No.2016-I2M-1-001), National Natural Science Foundation of China (No. 81472785).

Authors' contributions

YW designed and supervised the program. HL and YQ conducted the *in vitro* and *in vivo* experiments. NZ performed all the data analysis and bioinformatics analysis. The manuscript was produced by DM, HL and YQ, which was checked by YW All the authors approved the submission of this manuscript.

Acknowledgements

This study was financially supported by CAMS Initiative for Innovative Medicine, National Natural Science Foundation of China, CAMS Innovation Fund for Medical Sciences.

References

1. Siegel RL, Miller KD, Jemal A. Cancer statistics, 2020. CA-Cancer J. Clin. 2020; **70**, 7-30.

2. Bray F, Ferlay J, Soerjomataram I, Siegel RL, Torre LA, Jemal A. Global cancer statistics 2018: GLOBOCAN estimates of incidence and mortality worldwide for 36 cancers in 185 countries. CA-Cancer J. Clin. 2018; **68**, 394-424.
3. Ettinger DS, Wood DE, Aisner DL, Akerley W, Bauman J, Chirieac LR, et al. Non-Small Cell Lung Cancer, Version 5.2017, NCCN Clinical Practice Guidelines in Oncology. J. Natl. Compr. Canc. Ne. 2017; **15**, 504-535.
4. Petersen I, Warth A. Lung cancer: developments, concepts, and specific aspects of the new WHO classification. J. Cancer Res. Clin. 2016; **142**, 895-904.
5. Torre LA, Siegel RL, Jemal A. Lung Cancer Statistics. Adv Exp Med Biol. 2016; **893**, 1-19.
6. Walder D, O'Brien M. Looking back and to the future: Are we improving 'cure' in non-small cell lung cancer? Eur. J. Cancer 2017; **75**, 192-194.
7. Barr Kumarakulasinghe N, Zanwijk NV, Soo RA. Molecular targeted therapy in the treatment of advanced stage non-small cell lung cancer (NSCLC). Respirology. 2015; **20**, 370-378 (2015).
8. Rosell R, Karachaliou N. Adjuvant therapy for resected EGFR-mutant non-small-cell lung cancer. Lancet Oncol 2018; **19**, e126.
9. Wang J, Zhao X, Wang Y, Ren F, Sun D, Yan Y, et al. circRNA-002178 act as a ceRNA to promote PDL1/PD1 expression in lung adenocarcinoma. Cell Death Dis. 2020; **11**, 32.
10. Cai Y, Sheng Z, Chen Y, Wang J. LncRNA HMMR-AS1 promotes proliferation and metastasis of lung adenocarcinoma by regulating MiR-138/sirt6 axis. Aging. 2019; **11**, 3041-3054.
11. Brayer KJ, Segal DJ. Keep Your Fingers Off My DNA: Protein–Protein Interactions Mediated by C2H2 Zinc Finger Domains. Cell Biochem. Biophys. 2008; **50**, 111-131.
12. Jen J, Wang Y. Zinc finger proteins in cancer progression. J. Biomed. Sci. 2016; **23**, 53.
13. Beà S, Salaverria I, Armengol L, Pinyol M, Fernández V, Hartmann EM, et al. Uniparental disomies, homozygous deletions, amplifications, and target genes in mantle cell lymphoma revealed by integrative high-resolution whole-genome profiling. Blood. 2009; **113**, 3059.
14. Hamed MY, Arya G. Zinc finger protein binding to DNA: an energy perspective using molecular dynamics simulation and free energy calculations on mutants of both zinc finger domains and their specific DNA bases. J. Biomol. Struct. Dyn. 2016; **34**, 919-934.
15. Li Y, Yang Q, Guan H, Shi B, Ji M, Hou P. ZNF677 Suppresses Akt Phosphorylation and Tumorigenesis in Thyroid Cancer. Cancer Res. 2018; **78**, 5216.
16. Nie H, Mu J, Wang J, Li Y. miR-195-5p regulates multi-drug resistance of gastric cancer cells via targeting ZNF139. Oncol. Rep. 2018; **40**, 1370-1378.
17. Zhang X, Jiang G, Wu J, Zhou H, Zhang Y, Miao Y, et al. Zinc finger protein 668 suppresses non-small cell lung cancer invasion and migration by downregulating Snail and upregulating E-cadherin and zonula occludens-1. Oncol. Lett. 2018; **15**, 3806-3813.
18. Harada Y, Kanehira M, Fujisawa Y, Takata R, Shuin T, Miki T, et al. Cell-Permeable Peptide DEPDC1-ZNF224 Interferes with Transcriptional Repression and Oncogenicity in Bladder Cancer Cells. Cancer

Res. 2010; **70**, 5829.

19. Gomesduarte A, Lacerda R, Menezes J, Romão L. eIF3: a factor for human health and disease. RNA Biol. 2017; **15**, 26-34.
20. Lee ASY, Kranzusch PJ, Cate JHD. eIF3 targets cell-proliferation messenger RNAs for translational activation or repression. Nature. 2015; **522**, 111-114.
21. Valášek LS, et al. Embraced by eIF3: structural and functional insights into the roles of eIF3 across the translation cycle. Nucleic Acids Res. 2017; **45**, 10948-10968.
22. Hershey JWB. The role of eIF3 and its individual subunits in cancer. Biochim Biophys Acta. 2015; **1849**, 792-800.
23. Yin Y, Long J, Sun Y, Li H, Jiang E,Zeng C, et al. The function and clinical significance of eIF3 in cancer. Gene. 2018; **673**, 130-133.
24. Yin JY, Zhang JT, Zhang W, Zhou HH, Liu ZQ. eIF3a: A new anticancer drug target in the eIF family. Cancer Lett. 2018; **412**, 81-87.
25. Liu T, Wei Q, Jin J, Luo Q, Liu Y, Yang Y, et al. The m6A reader YTHDF1 promotes ovarian cancer progression via augmenting EIF3C translation. Nucleic Acids Res. 2020; **DOI: 10.1093/nar/gkaa048**,.
26. Wen F, Wu ZY, Nie L, Zhang QZ, Qin YK, Zhou Z, et al. Eukaryotic initiation factor 3, subunit C silencing inhibits cell proliferation and promotes apoptosis in human ovarian cancer cells. Bioscience Rep. 2019; **39**, BSR20191124.
27. Fan M, Wang K, Wei X, Yao H, Chen Z, He X. Upregulated expression of eIF3C is associated with malignant behavior in renal cell carcinoma. Int. J. Oncol. 2019; **55**, 1385-1395.
28. Gao W, Hu Y, Zhang Z, Du G, Yin L, Yin Z. Knockdown of EIF3C promotes human U-2OS cells apoptosis through increased CAS P3/7 and Chk1/2 by upregulating SAPK/JNK. OncoTargets Ther. 2019; **12**, 1225-1235.
29. Hu C, Yue W, Ao L, Jin Z, Fangfang X, Li Z. Overexpressed circ_0067934 acts as an oncogene to facilitate cervical cancer progression via the miR-545/EIF3C axis. J. Cell. Physiol. 2018; **234**, 9225-9232.

Supplementary Figure Legends

Figure S1. The transfection efficiencies of shZNF280A and shCtrl in A549 and NCI-H1299 cells were evaluated through observing the fluorescence of GFP on lentivirus vector.

Figure S2. Human Apoptosis Antibody Array was performed to detect and compare the expression of apoptosis-related proteins in NCI-H1299 cells with or without ZNF280A knockdown.

Figure S3. (A) A PrimeView Human Gene Expression Array was performed to identify the differentially expressed genes (DEGs) between shZNF280A and shCtrl groups of NCI-H1299 cells. (B) The volcano plot of gene expression profiling in NCI-H1299 cells with or without ZNF280A knockdown. Green dots represent the downregulated DEGs, red dots represent the upregulated DEGs. (C) The enrichment of the

DEGs in canonical signaling pathways was analyzed by IPA. (D) The enrichment of the DEGs in IPA disease and function was analyzed by IPA.

Figure S4. (A) The knockdown efficiencies of 3 shRNAs prepared for silencing EIF3C were evaluated through qPCR. (B) The transfection efficiencies of shEIF3C and shCtrl in NCI-H1299 cells were evaluated through observing the fluorescence of GFP on lentivirus vector. ** $P < 0.01$

Figure S5. (A) The transfection efficiencies of Control plasmid and ZNF280A overexpression plasmid were evaluated through observing the fluorescence of GFP on lentivirus vector. (B, C) The overexpression of ZNF280A in NCI-H1299 was confirmed by qPCR (B) and western blotting (C), respectively. *** $P < 0.001$

Figure S6. (A) The transfection efficiencies of NC(OE+KD) and ZNF280A+shEIF3C in NCI-H1299 cells were evaluated through observing the fluorescence of GFP on lentivirus vector. (B) The mRNA and protein levels of ZNF280A and EIF3C in NCI-H1299 cells transfected with different plasmids were detected by qPCR and western blotting, respectively. Data was shown as mean ± SD. * $P < 0.05$, ** $P < 0.01$

Figures

Figure 1

ZNF280A was upregulated in LUAD tissues and expressed in LUAD cells. (A) The expression level of ZNF280A was detected by IHC analysis in LUAD tissues and normal tissues. (B) The Kaplan-Meier survival analysis showed the significant association between ZNF280A high expression and shorter survival period of LUAD patients. (C) The mRNA expression of ZNF280A in A549, NCI-H1299 and SPC-A-1 cell lines was detected by qPCR. Data was shown as mean ± SD. *P < 0.05, **P < 0.01, ***P < 0.001

Figure 2

ZNF280A knockdown inhibited LUAD development in vitro. (A, B) Cell models with or without ZNF280A knockdown were constructed by infecting shZNF280A or shCtrl. The knockdown efficiency of ZNF280A in A549 and NCI-H1299 cells was assessed by qPCR and western blotting, respectively. (B) MTT assay was employed to show the effects of ZNF280A on cell proliferation of A549 and NCI-H1299 cells. (C) Flow cytometry was performed to detect cell apoptosis of A549 and NCI-H1299 cells with or without ZNF280A knockdown. (D) Cell cycle distribution was estimated in A549 and NCI-H1299 cells with or without ZNF280A knockdown. (E, F) The effects of ZNF280A on cell migration ability of A549 and NCI-H1299 cells were evaluated by wound-healing assay (E) and Transwell assay (F). The representative images were selected from at least 3 independent experiments. Data was shown as mean ± SD. *P < 0.05, **P < 0.01, ***P < 0.001

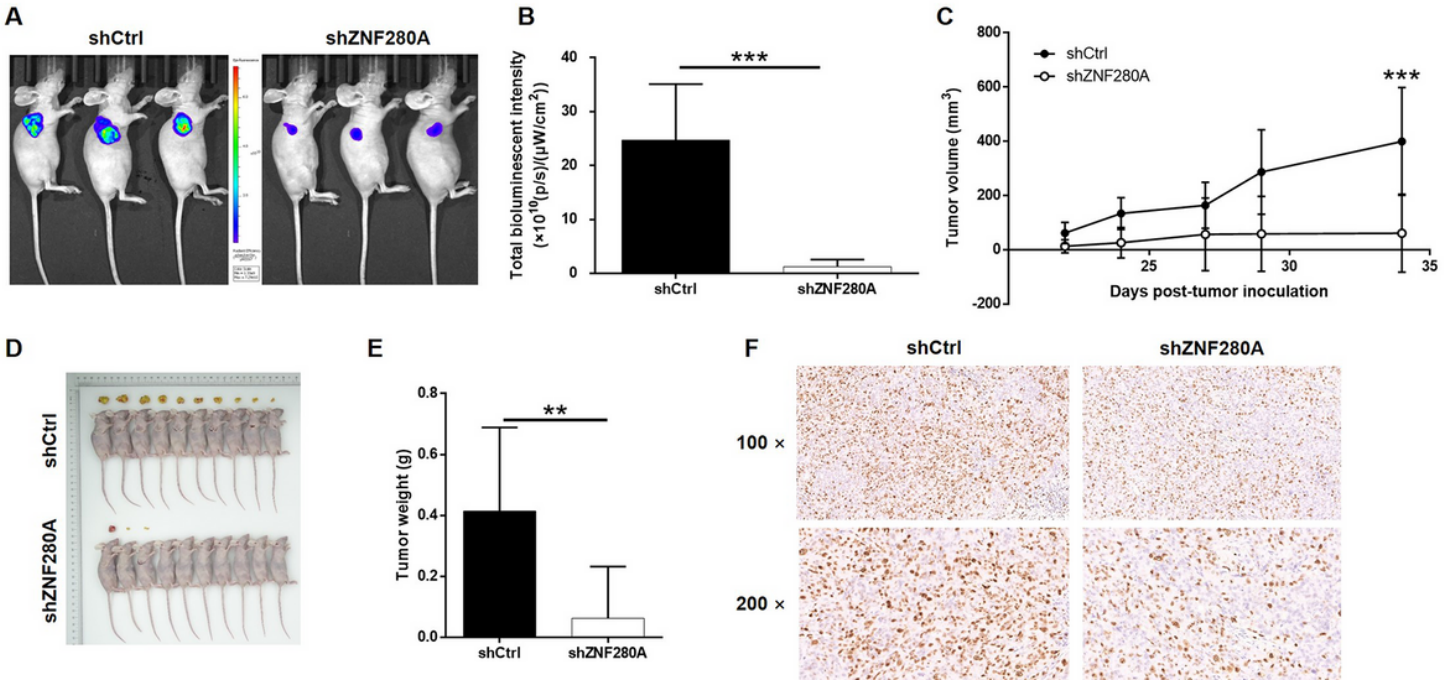

Figure 3

ZNF280A knockdown inhibited LUAD development in vivo. (A) 22 days post injection of NCI-H1299 cells with or without ZNF280A knockdown, the volume of tumors formed in mice was measured and calculated at indicated time intervals. (B) In vivo imaging was performed to evaluate the tumor burden in mice of shZNF280A and shCtrl groups at day 34 post tumor-inoculation. (C) The bioluminescence intensity was scanned and used as a representation of tumor burden in mice of shZNF280A and shCtrl groups. (D, E) Mice were sacrificed at day 34 post injection, and the tumors were removed for collecting photos (D) and weighing (E). (F) The expression of Ki67 in sections of xenografts was detected by IHC analysis. Data was shown as mean ± SD. *P < 0.05, **P < 0.01, ***P < 0.001

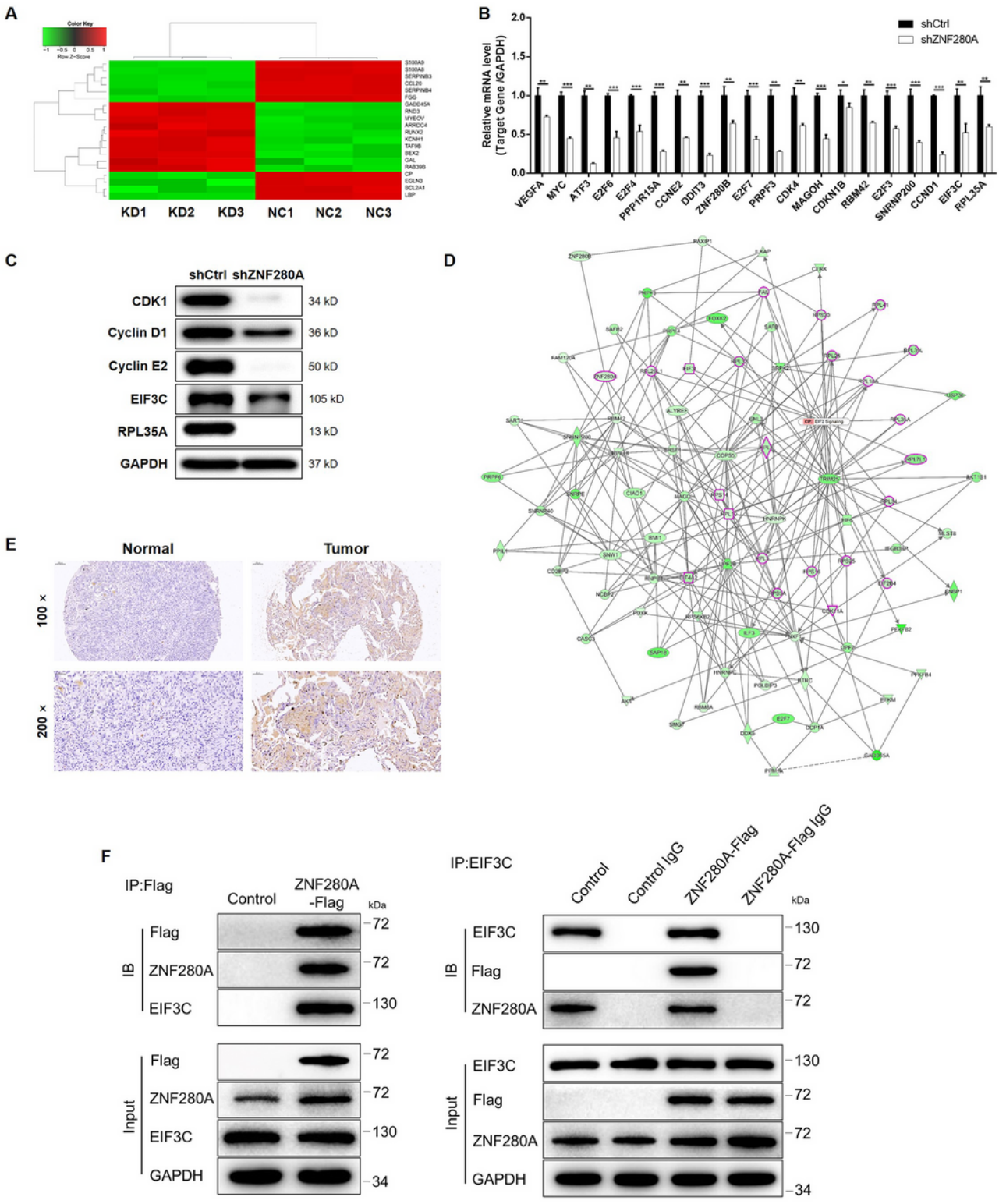

Figure 4

The exploration and verification of downstream underlying ZNF280A induced regulation of LUAD. (A) A PrimeView Human Gene Expression Array was performed to identify the differentially expressed genes (DEGs) between shZNF280A and shCtrl groups of NCI-H1299 cells. (B, C) qPCR (B) and western blotting (C) were used to detect the expression of several selected DEGs in NCI-H1299 cells with or without ZNF280A. (D) A ZNF280A associated interaction network constructed by IPA analysis revealed the

potential linkage between ZNF280A and EIF3C. (E) The expression of EIF3C in LUAD tissues and normal tissues was evaluated by IHC analysis. (F) The direct interaction between ZNF280A and EIF3C was proved by co-immunoprecipitation. Data was shown as mean ± SD. *P < 0.05, **P < 0.01, ***P < 0.001

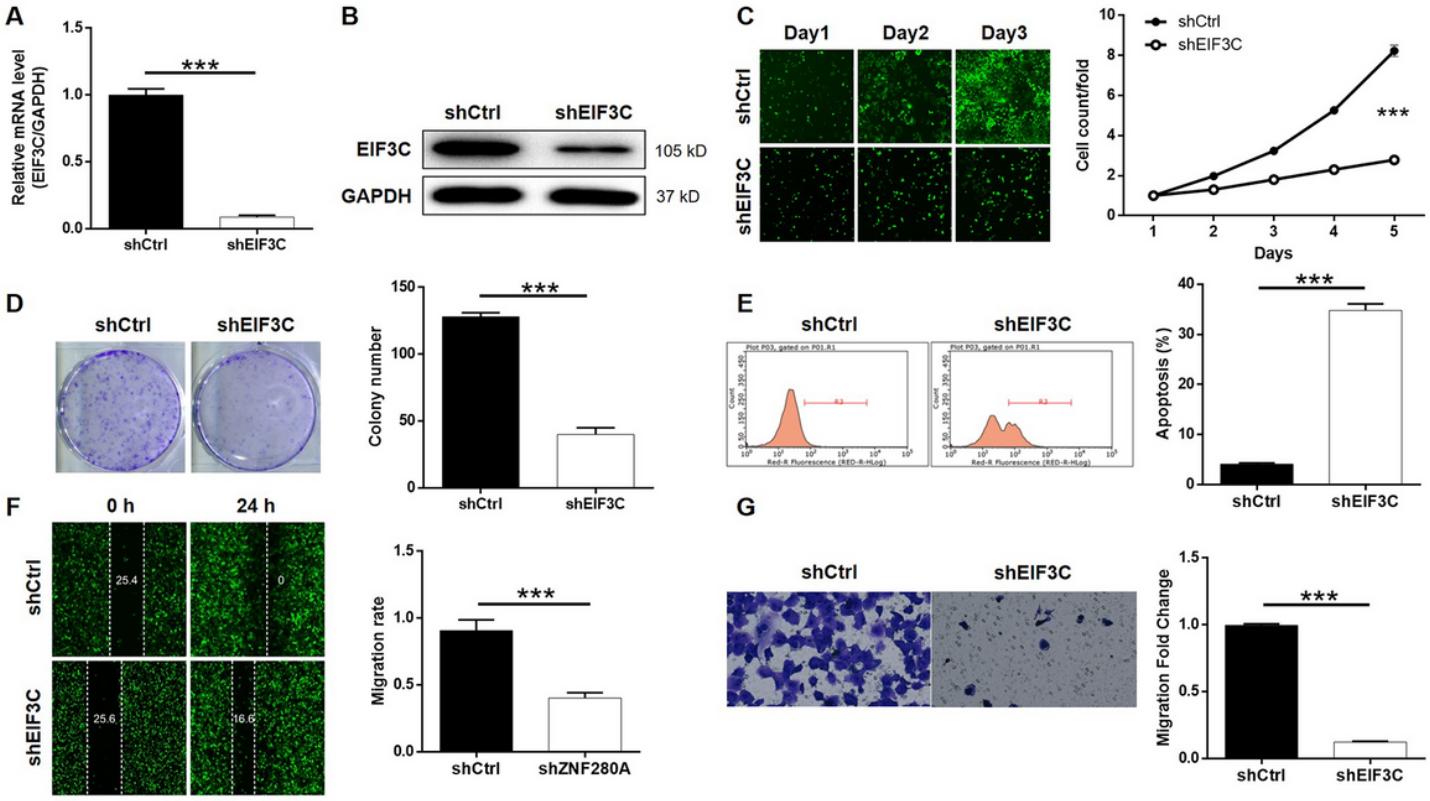

Figure 5

EIF3C knockdown inhibited LUAD development in vitro. (A, B) Cell models with or without EIF3C knockdown were constructed. The knockdown efficiency of EIF3C in NCI-H1299 cells was assessed by qPCR (A) and western blotting (B), respectively. (C) Celigo cell counting assay was employed to show the effects of EIF3C on cell proliferation of NCI-H1299 cells. (D) Colony formation assay was used to evaluate the ability of NCI-H1299 cells with or without EIF3C knockdown to form colonies. (E) Flow cytometry was performed to detect cell apoptosis of NCI-H1299 cells with or without EIF3C knockdown. (F, G) The effects of EIF3C on cell migration ability of NCI-H1299 cells were evaluated by wound-healing assay (F) and Transwell assay (G). The representative images were selected from at least 3 independent experiments. Data was shown as mean ± SD. *P < 0.05, **P < 0.01, ***P < 0.001

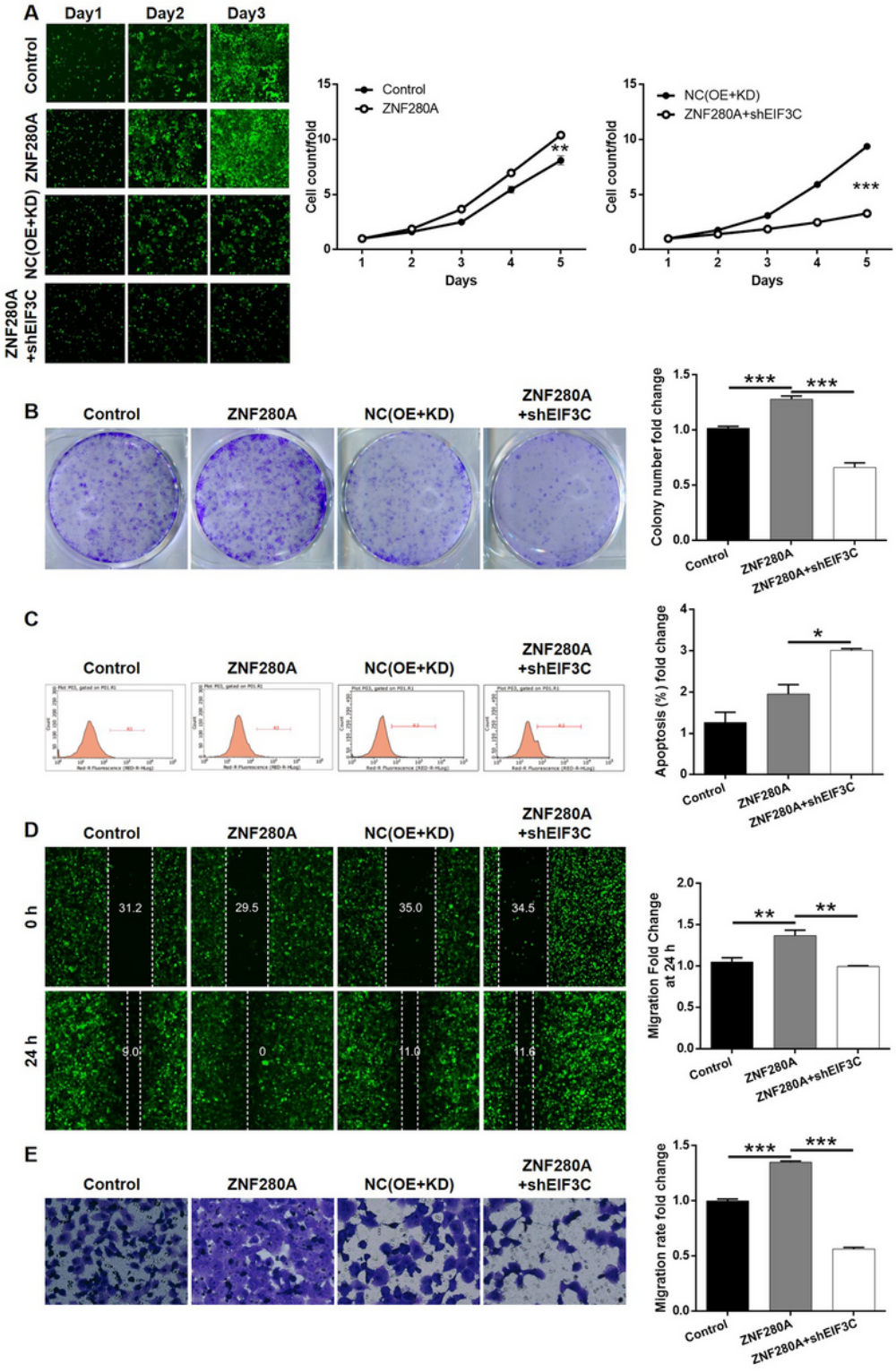

Figure 6

Knockdown of EIF3C attenuated the effects of LUAD cells by ZNF280A overexpression. NCI-H1299 cells transfected with Control plasmids, ZNF280A overexpression plasmids, NC(OE+KD), and simultaneous ZNF280A overexpression plasmids and shEIF3C were subjected to the detection of cell proliferation by Celigo cell counting assay (A), colony formation (B), cell apoptosis by flow cytometry (C), cell migration by wound-healing assay (D) and cell migration by Transwell assay (E). The representative images were

selected from at least 3 independent experiments. Data was shown as mean ± SD. *P < 0.05, **P < 0.01, ***P < 0.001

Supplementary Files

This is a list of supplementary files associated with this preprint. Click to download.

- TableS1.docx
- FigureS2.tif
- FigureS1.tif
- FigureS4.tif
- FigureS3.tif
- FigureS6.tif
- FigureS5.tif
- TableS4.docx
- TableS3.docx
- TableS2.docx